

# Microwave $TM_{010}$ cavities as versatile 4D electron optical elements

P.L.E.M. Pasmans\*, G.B. van den Ham, S.F.P. Dal Conte, S.B. van der Geer, O.J. Luiten

Eindhoven University of Technology, P.O. Box 513, 5600 MB Eindhoven, The Netherlands

## ARTICLE INFO

Available online 27 July 2012

### Keywords:

Ultrafast electron diffraction  
Electron optics  
Resonant microwave cavities

## ABSTRACT

The realization of high quality ultrashort pulsed beams requires ultrafast time-dependent electron optics. We present derivations of closed expressions both for the longitudinal and transverse focusing powers of resonant microwave  $TM_{010}$  cavities. The derived expressions are validated by particle tracking simulations using realistic cavity fields. For small field amplitudes, in which case the “weak lens” approximation holds, the focusing powers obtained from simulations are in good agreement with the derived expressions. Furthermore, the required phase and temperature stability for synchronization of electron bunches generated by femtosecond photoemission are discussed.

© 2012 Elsevier B.V. All rights reserved.

## 1. Introduction

Electron microscopes have pushed spatial resolutions down to the sub-Å level, making it possible to resolve and even identify individual atoms [1]. High resolution electron microscopy is, however, restricted almost exclusively to the study of equilibrium structures, since the timescales associated with the motion of individual atoms can be as short as 100 fs, i.e. many orders of magnitude faster than typical electron microscopy exposure times. The challenge ahead is to resolve this atomic motion, both in time and space (4D), enabling the study of structural dynamics of, e.g., chemical reactions, phase transitions, and conformational changes at the most fundamental level.

In recent years, the implementation of femtosecond laser photoemission to generate ultrashort electron bunches has led to exciting progress in this direction [2–8]. Technological developments, however, have mainly been focused on ultrafast *source* development. The realization of high quality ultrashort pulsed beams also requires ultrafast time-dependent electron *optics* to overcome limitations due to space charge effects [9–12]. Recently, it has been demonstrated that a  $TM_{010}$  cavity can be used to compress electron bunches down to sub-100 fs bunch durations [13,14]. Bunch compression can be regarded as longitudinal focusing. Clearly, by using a  $TM_{010}$  cavity as a longitudinal focusing element, it can also serve to manipulate the energy spread of an electron bunch. Moreover, phase space manipulation with a  $TM_{010}$  resonant microwave cavity is not restricted to longitudinal degrees of freedom only. As already studied during the 1960s and 1970s [15,16], resonant microwave cavities can be

used as time-dependent lenses – i.e. transverse focusing elements – as well. Since Scherzer’s theorem [17] does not apply for time-dependent optics, cavity lenses can in principle be used for correction of spherical aberration. In addition, they may also be used for correction of chromatic aberration [15]. The use of cavity lenses as correcting elements would require a pulsed electron beam. This could be accomplished by using another microwave cavity as a beam chopper.

In this paper, we present derivations of closed expressions both for the longitudinal and the transverse focusing powers of  $TM_{010}$  cavities, which are valid at relativistic speeds as well. The use of microwave cavities as electron lenses has been studied extensively before [15,16]. Here, we present a compact derivation of the most essential closed expressions for the focusing powers and validate the applicability and accuracy of the derived equations by particle tracking simulations using realistic cavity fields. These expressions provide valuable insight into the beam dynamics and they are useful tools for designing beam lines. Synchronization of the arrival of electron bunches at the desired radio frequency (RF) phase of the field in the cavity is crucial. We discuss the required phase and temperature stability for synchronization of electron bunches generated by femtosecond photoemission.

## 2. Longitudinal and transverse focusing powers – analytical theory

### 2.1. Framework and assumptions

In this section, closed expressions are derived both for the transverse and the longitudinal focusing powers of an electron bunch passing through a resonant microwave cavity oscillating in the  $TM_{010}$  mode. For this rotationally symmetric mode, we

\* Corresponding author. Tel.: +31 40 2474355.

E-mail address: [p.l.e.m.pasmans@tue.nl](mailto:p.l.e.m.pasmans@tue.nl) (P.L.E.M. Pasmans).

describe the electromagnetic field in cylindrical coordinates  $(r, \varphi, z)$ . As derived in the Appendix, for a rotationally symmetric mode, the oscillating electric field  $\vec{E}(\vec{r}, t) \equiv \vec{E}_0(\vec{r}) \cos(\omega t + \phi_0)$  and magnetic field  $\vec{B}(\vec{r}, t)$  can be expanded in a power series in  $r$ , with coefficients that only depend on the on-axis electric field amplitude  $E_{0,z}(r=0, \phi=0, z) \equiv E_{0,z}(z)$

$$E_z(\vec{r}, t) = \left(1 - \frac{r^2}{4} \left\{ \frac{\partial^2}{\partial z^2} + \frac{\omega^2}{c^2} \right\} + \dots\right) E_{0,z}(z) \cos(\omega t + \phi_0) \quad (1)$$

$$E_r(\vec{r}, t) = \left(-\frac{r}{2} + \frac{r^3}{16} \left\{ \frac{\partial^2}{\partial z^2} + \frac{\omega^2}{c^2} \right\} - \dots\right) \frac{\partial E_{0,z}(z)}{\partial z} \cos(\omega t + \phi_0) \quad (2)$$

$$B_\varphi(\vec{r}, t) = \left(-\frac{r}{2} + \frac{r^3}{16} \left\{ \frac{\partial^2}{\partial z^2} + \frac{\omega^2}{c^2} \right\} - \dots\right) E_{0,z}(z) \frac{\omega}{c^2} \sin(\omega t + \phi_0) \quad (3)$$

where the electromagnetic field oscillates at an angular frequency  $\omega$  with a phase offset  $\phi_0$ . The center of the electron bunch is traveling along the symmetry axis ( $r=0$ ) in the (positive)  $z$ -direction. The radial electron coordinate  $\rho$  and the longitudinal electron coordinate  $\zeta$  are defined in the co-moving frame with respect to the center of the electron bunch. The time  $t$  is defined such that the center of the electron bunch ( $\rho=0, \zeta=0$ ) is at the center of the cavity ( $r=0, z=0$ ) at  $t=0$ .

To derive the focusing powers, the following assumptions are made:

- The transverse size of the bunch is considered to be sufficiently small so that only the first order terms need to be taken into account.
- The duration of the bunch is much shorter than the period of the oscillating electromagnetic field in the cavity ( $\zeta \ll v_z/\omega$ ).
- The positions of the electrons ( $\rho, \zeta$ ) with respect to the center of the bunch are assumed to be constant during passage through the cavity.
- The change in momentum during passage through the cavity is small,  $\Delta p_r, \Delta p_z \ll p_z$ , so the velocity  $v_z$  of the electron bunch is approximately constant, implying  $\zeta \cong z - v_z t$  and  $\rho \cong r$ .

Basically, (a) is the usual paraxial approximation and (b) is its longitudinal equivalent. Analogously, (c) is the usual thin lens approximation and (d) is the weak lens approximation.

## 2.2. Transverse focusing power

To determine the transverse focusing power, the change of the transverse momentum  $\Delta p_r$  of an electron passing through the cavity is calculated, analogous to [18]

$$\Delta p_r = -e \int_{-\infty}^{\infty} (\vec{E} + \vec{v} \times \vec{B}) \cdot \vec{e}_r dt = -e \int_{-\infty}^{\infty} (E_r - v_z B_\varphi) dt \quad (4)$$

Applying assumptions (a) and (d), and using  $t=z/v_z$ ,  $\Delta p_r$  becomes

$$\Delta p_r \cong -e \frac{\rho}{2} \int_{-\infty}^{\infty} \left[ -\frac{1}{v_z} \frac{\partial E_{0,z}(z)}{\partial z} \cos\left(\omega \frac{z}{v_z} + \phi_0\right) + \frac{\omega}{c^2} E_{0,z}(z) \sin\left(\omega \frac{z}{v_z} + \phi_0\right) \right] dz \quad (5)$$

By partial integration of the first term of the integrand and by using  $E_{0,z}(0, \pm\infty)=0$ , Eq. (5) can be rewritten as

$$\Delta p_r \cong e \frac{\rho}{2} \frac{\omega}{\gamma^2 v_z^2} \int_{-\infty}^{\infty} E_{0,z}(z) \left[ \cos\left(\omega \frac{z}{v_z}\right) \sin(\phi_0) + \sin\left(\omega \frac{z}{v_z}\right) \cos(\phi_0) \right] dz \quad (6)$$

where we have used  $\gamma = (1 - (v/c)^2)^{-1/2} \cong (1 - (v_z/c)^2)^{-1/2}$ . For a cavity oscillating in the  $\text{TM}_{010}$  mode,  $E_{0,z}$  is an even function of  $z$  therefore the right term between brackets in Eq. (6) cancels out after integration. Furthermore, an effective cavity length is defined as

$$d_c \equiv \int_{-\infty}^{\infty} [E_{0,z}(z)/E_0] \cos\left(\omega \frac{z}{v_z}\right) dz \quad (7)$$

where  $E_0 \equiv E_{0,z}(z=0)$ . By dropping the right term between brackets in Eq. (6) and using definition (7),  $\Delta p_r$  becomes

$$\Delta p_r \cong e \frac{\rho}{2} \frac{\omega}{\gamma^2 v_z^2} E_0 d_c \sin \phi_0 \quad (8)$$

The transverse focusing power  $P_T$  (or the inverse of the transverse focal length  $f_T$ ) is defined as

$$P_T = \frac{1}{f_T} \equiv -\frac{1}{v_z} \frac{\partial \Delta v_r}{\partial \rho} = -\frac{1}{v_z} \frac{1}{\gamma m_e} \frac{\partial \Delta p_r}{\partial \rho} \quad (9)$$

Combining Eqs. (8) and (9), we finally arrive at

$$P_T = -\frac{e E_0 d_c \omega}{2 m_e \gamma^3 v_z^3} \sin \phi_0 \quad (10)$$

## 2.3. Longitudinal focusing power

To determine the longitudinal focusing power, the change of the longitudinal momentum  $\Delta p_z$  of an electron passing through the cavity is calculated

$$\Delta p_z = -e \int_{-\infty}^{\infty} (\vec{E} + \vec{v} \times \vec{B}) \cdot \vec{e}_z dt = -e \int_{-\infty}^{\infty} E_z dt \quad (11)$$

Applying assumptions (a) and (d), and using  $t=(z-\zeta)/v_z$ , we find

$$\Delta p_z \cong -\frac{e}{v_z} \int_{-\infty}^{\infty} E_{0,z}(z) \left[ \cos\left(\omega \frac{z}{v_z}\right) \cos\left(-\omega \frac{\zeta}{v_z} + \phi_0\right) - \sin\left(\omega \frac{z}{v_z}\right) \sin\left(-\omega \frac{\zeta}{v_z} + \phi_0\right) \right] dz \quad (12)$$

For a cavity oscillating in the  $\text{TM}_{010}$  mode,  $E_{0,z}$  is an even function of  $z$  therefore the right term between brackets in Eq. (12) does not contribute. Applying assumptions (b) and (c), Eq. (12) can be rewritten as

$$\Delta p_z \cong -\frac{e E_0 d_c}{v_z} \left( \omega \frac{\zeta}{v_z} \sin \phi_0 + \cos \phi_0 \right) \quad (13)$$

In analogy with the definition of  $P_T$ , the longitudinal focusing power  $P_L$  (or the inverse of the longitudinal focal length  $f_L$ ) is defined as

$$P_L = \frac{1}{f_L} \equiv -\frac{1}{v_z} \frac{\partial \Delta v_z}{\partial \zeta} = -\frac{1}{v_z} \frac{1}{\gamma^3 m_e} \frac{\partial \Delta p_z}{\partial \zeta} \quad (14)$$

Combining Eqs. (13) and (14), we finally arrive at

$$P_L = \frac{e E_0 d_c \omega}{m_e \gamma^3 v_z^3} \sin \phi_0 \quad (15)$$

It is interesting to note that the transverse focusing power is simply related to the longitudinal focusing power by a factor minus one half,  $P_T = -P_L/2$ . For non-relativistic speeds, this can be easily explained. If  $v_z \ll c$ , the contribution of the magnetic field in Eq. (4) can be neglected. From the fact that the electric field is divergence free,  $\partial E_z/\partial z \cong -2\partial E_r/\partial r$ , it then directly follows that  $P_T = -P_L/2$ .

### 3. Particle tracking simulations

#### 3.1. Simulation settings

Strictly speaking, the closed expressions (10) and (15) derived for  $P_T$  and  $P_L$  only hold in the “paraxial” approximations (a) and (b), the “thin lens” approximation (c), and the “weak lens” approximation (d). Here, we test the validity of the closed expressions by means of particle tracking simulations for electron bunch and cavity field parameters, which could be used in an actual electron diffraction setup. The simulations are performed using the General Particle Tracer (GPT) code [19]. The exact fields of the  $TM_{010}$  cavity which is described in [13,14], are used in the simulations. For this cavity, the resonant frequency  $\omega/2\pi=3$  GHz, and the effective cavity length  $d_c=6$  mm; its field profile is shown in Fig. 1. In the simulations, the electron bunches entering the cavity have an energy of 100 keV, an RMS width  $\sigma_r=100$   $\mu\text{m}$ , and an RMS duration  $\sigma_t=1$  ps. The beam entering the cavity is perfectly parallel, with zero emittance, and Coulomb interactions between the electrons are not taken into account.

#### 3.2. Results and discussion

In Fig. 2, the longitudinal focusing power derived from GPT simulations is compared with the focusing power predicted by

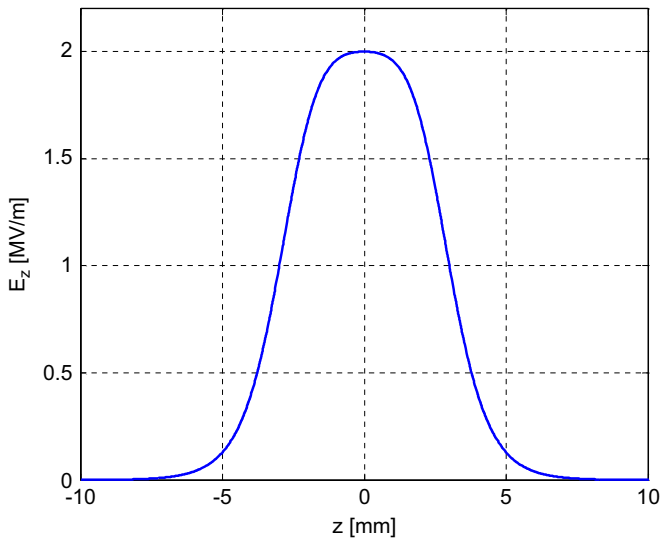


Fig. 1. The  $TM_{010}$  field profile used in the simulations. For this field profile, the effective cavity length  $d_c=6$  mm.

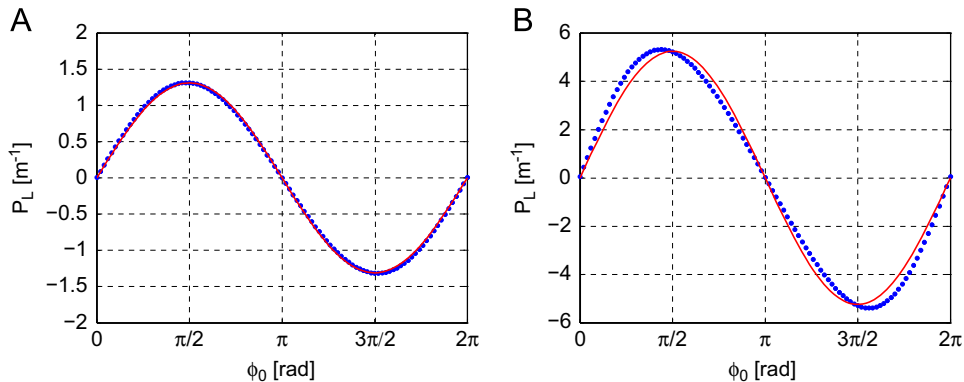


Fig. 2. Longitudinal focusing power ( $P_L$ ) versus phase offset ( $\varphi_0$ ) for field amplitudes  $E_0=0.5$  MV/m (A) and  $E_0=2$  MV/m (B). The theoretical values are indicated by the red solid curve and the simulated values by blue dots. (For interpretation of the references to color in this figure caption, the reader is referred to the web version of this article.)

Eq. (15). Simulations have been performed for phase offsets  $\varphi_0$  ranging from 0 to  $2\pi$  and for field amplitudes  $E_0=0.5$  MV/m (Fig. 2A) and  $E_0=2$  MV/m (Fig. 2B). For a field amplitude  $E_0=0.5$  MV/m, the simulated curve of the focusing power is in good agreement with the theoretical curve. In this case, the maximal increase in kinetic energy for an electron passing through the cavity is 3 keV, i.e. 3% of the initial kinetic energy. For a field amplitude  $E_0=2$  MV/m, both curves qualitatively still follow the same trend, but the values of the focusing power clearly start to deviate and the maximum and minimum in focusing power have shifted to other values of  $\varphi_0$ . The deviations can be explained as follows. For phase offsets  $0 < \varphi_0 < \pi/2$  and  $3\pi/2 < \varphi_0 < 2\pi$ , the cavity induces a net deceleration of the electron bunch – see Eq. (13) – and the focusing effect becomes stronger. For phase offsets  $\pi/2 < \varphi_0 < 3\pi/2$ , the cavity induces a net acceleration of the electron bunch and the focusing effect becomes weaker. For a field amplitude  $E_0=2$  MV/m, the maximal increase in kinetic energy is 12 keV, i.e. 12% of the initial kinetic energy. In this case, the “thin lens” and “weak lens” approximations (c) and (d) are no longer strictly valid.

For the transverse focusing power, shown in Fig. 3, similar observations as for the longitudinal focusing power can be made. For a field amplitude  $E_0=0.5$  MV/m (Fig. 3A), the simulated and theoretical curves are in good agreement. For a field amplitude  $E_0=2$  MV/m (Fig. 3B), assumptions (c) and (d) are no longer strictly valid, and the curves show a clear discrepancy.

Figs. 4 and 5 show the longitudinal and transverse focusing powers, respectively, as a function of field amplitude  $E_0$  at a fixed phase offset  $\varphi_0=\pi/2$ . The theoretical curves are in good agreement with the simulated curves. Only for the highest field strengths ( $E_0=4$  MV/m) the theoretical and simulated values start to deviate slightly. As before, for these highest field strengths, assumptions (c) and (d) are no longer strictly valid.

### 4. Practical realization

Until now, we have discussed theoretical aspects of using a  $TM_{010}$  cavity as a lens element in an electron microscope. In this section, some practical aspects are discussed.

#### 4.1. Applications

A  $TM_{010}$  cavity can serve as a transverse focusing element with the unique property that it can both have a convergent and a divergent effect, whereas a conventional lens formed by either an electrostatic or a magnetostatic field that is rotationally symmetric, can only have a convergent net effect [15]. In addition, it

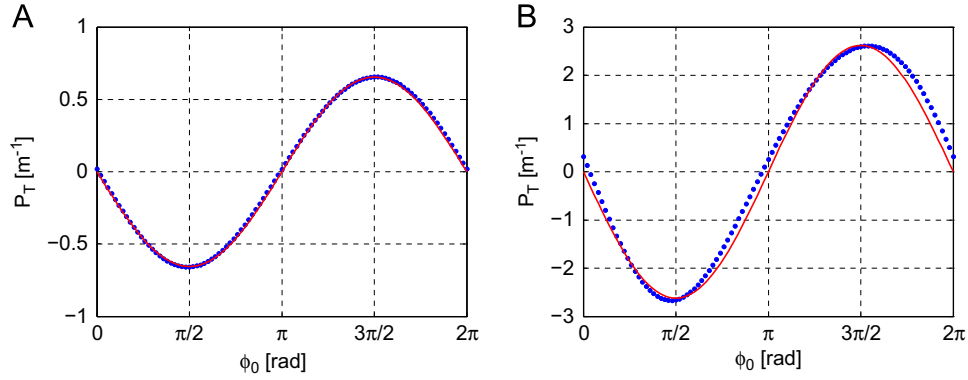


**Fig. 3.** Transverse focusing power ( $P_T$ ) versus phase offset ( $\phi_0$ ) for field amplitudes  $E_0=0.5$  MV/m (A) and  $E_0=2$  MV/m (B). The theoretical values are indicated by the red solid curve and the simulated values by blue dots. (For interpretation of the references to color in this figure caption, the reader is referred to the web version of this article.)

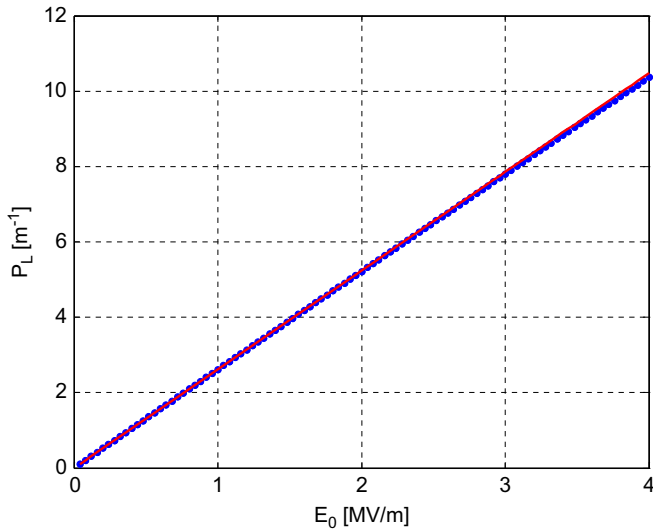


**Fig. 4.** Longitudinal focusing power ( $P_L$ ) versus field amplitude ( $E_0$ ) for a fixed phase offset  $\phi_0=\pi/2$ . The theoretical values are indicated by the red solid curve and the simulated values by blue dots. (For interpretation of the references to color in this figure caption, the reader is referred to the web version of this article.)

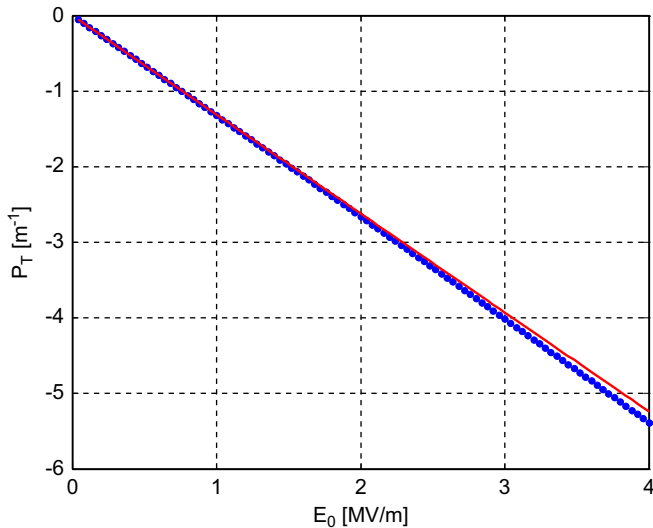


**Fig. 5.** Transverse focusing power ( $P_T$ ) versus field amplitude ( $E_0$ ) for a fixed phase offset  $\phi_0=\pi/2$ . The theoretical values are indicated by the red solid curve and the simulated values by blue dots. (For interpretation of the references to color in this figure caption, the reader is referred to the web version of this article.)

may be used as a longitudinal focusing element which gives control over the duration and energy distribution of an electron bunch. The cavity could in principle also be used for (additional) acceleration of an electron bunch.

Moreover, as stated by Scherzer's theorem [17], a conventional static lens with a rotationally symmetric field always has a positive coefficient of spherical aberration. For time-dependent electromagnetic fields, this restriction is lifted. By making use of the change in field direction while the electron bunch is in the cavity, it is possible to correct both spherical and chromatic aberrations [15].

In the economic and energy efficient  $\text{TM}_{010}$  cavity developed in our group [13,14] for ultrafast electron diffraction experiments, a field amplitude  $E_0=2$  MV/m is obtained for 43 W of RF power. In combination with an effective cavity length  $d_c=6$  mm, this corresponds to  $(\Delta U)_{\max}=eE_0d_c=12$  keV. For electrons with a kinetic energy  $U=100$  keV and in case of optimal bunch compression ( $\phi_0=\pi/2$ ), this cavity has a theoretical longitudinal focusing power  $P_L=5.2$   $\text{m}^{-1}$  (i.e.  $f_L=0.2$  m) and a transverse focusing power  $P_T=-2.6$   $\text{m}^{-1}$  (i.e.  $f_T=-0.4$  m). With an RF power of 1 kW, a field amplitude  $E_0=9.7$  MV/m can be achieved, which leads to theoretical focusing powers  $P_L=26$   $\text{m}^{-1}$  (i.e.  $f_L=0.04$  m) and  $P_T=-13$   $\text{m}^{-1}$  (i.e.  $f_T=-0.08$  m).

It is instructive to compare the focusing power of a  $\text{TM}_{010}$  cavity with the focusing power of a conventional solenoidal magnetic lens, which is given by

$$P_{\text{solenoid}} = \frac{e^2 \int_{-\infty}^{\infty} B_z(0,z)^2 dz}{4\gamma^2 m_e^2 v_z^2} \quad (16)$$

Comparing Eq. (16) with Eqs. (10) and (15), it is interesting to note that the focusing power of the cavity scales linearly with the electric field amplitude, whereas the focusing power of the solenoid scales quadratically with the magnetic field amplitude. The dependence on longitudinal momentum of the electrons is given by  $P \sim (\gamma v_z)^{-3} \sim p_z^{-3}$  for the cavity and  $P \sim (\gamma v_z)^{-2} \sim p_z^{-2}$  for the solenoid.

A coil with  $N_w$  windings and radius  $R$ , carrying a current  $I_w$ , can be modeled by a single current loop with a similar radius and carrying a current  $I=N_w I_w$ . In this case, Eq. (16) becomes

$$P_{\text{solenoid}} = \frac{3\pi}{128} \frac{e^2 \mu_0^2 I^2}{R \gamma^2 m_e^2 v_z^2} \quad (17)$$

For electrons with  $U=100$  keV, to achieve a focusing power of  $P_{\text{solenoid}}=2.6$   $\text{m}^{-1}$ , equivalent to the transverse focusing power of the  $\text{TM}_{010}$  cavity described above, a solenoid is required with, e.g.,  $R=5$  cm and  $I=N_w I_w=1.2$  kA.

## 4.2. Emittance and space charge

The minimum bunch dimensions that can be obtained using a microwave cavity (or any other type of lens) will be limited due to their emittance and space charge forces. A detailed discussion of emittance and space charge is beyond the scope of this paper. Here, we present simple estimates to determine what minimum bunch dimensions can be achieved for realistic bunch parameters in an ultrafast electron diffraction experiment. More accurate numbers can be obtained using semi-analytical approaches [9–12] or particle tracking simulations [19].

In the absence of space charge forces, the focal spot size is determined by the emittance of the beam and the focusing angle. The emittance  $\varepsilon_x$  is a measure for the focusability of the beam and thereby a measure of the beam quality [20]. The smaller the emittance becomes, the tighter is the focus that can be obtained. The normalized emittance is a Lorentz invariant measure of the focusability and is defined as  $\varepsilon_{n,x} = \gamma\beta\varepsilon_x$ . From Eqs. (8) and (10) we can derive that  $\Delta p_r = -p_z P_T \rho$  and from Eqs. (13) and (15) we can derive that  $\Delta p_z = -\gamma^2 p_z P_L \zeta$ . Given the normalized RMS emittances  $\varepsilon_{n,x}$  and  $\varepsilon_{n,z}$  and the initial RMS bunch dimensions  $\sigma_{x,i}$  and  $\sigma_{z,i}$ , we can determine the focal spot sizes  $\sigma_{x,0}$  and  $\sigma_{z,0}$  as a function of the focusing power

$$\sigma_{x,0} \cong \frac{\varepsilon_{n,x}}{\gamma\beta\sigma_{x,i}P_T} \quad (18)$$

$$\sigma_{z,0} \cong \frac{\varepsilon_{n,z}}{\gamma^3\beta\sigma_{z,i}P_L} \quad (19)$$

For a 100 keV electron bunch with  $\varepsilon_{n,x} = \varepsilon_{n,z} = 20$  nm rad [13] and  $\sigma_{x,i} = \sigma_{z,i} = 1$  mm, the achievable focal spot sizes are  $\sigma_{x,0} \sim 6$   $\mu\text{m}$  for  $P_T = 5$   $\text{m}^{-1}$  and  $\sigma_{z,0} \sim 4$   $\mu\text{m}$  for  $P_L = 5$   $\text{m}^{-1}$ .

To estimate the bunch charges for which space charge effects become dominant, we can consider the average potential energy per particle due to space charge forces of a uniformly filled sphere with radius  $R$  and with  $N$  electrons, given by [13]

$$\langle U_{p,disk} \rangle = \frac{3Ne^2}{20\pi\epsilon_0 R} \quad (20)$$

where  $\epsilon_0$  is the permittivity of vacuum. The average change in kinetic energy of a particle after passing through the cavity is approximately

$$\langle \Delta E_k \rangle_T = \frac{\langle \Delta p_x^2 \rangle}{2m} \cong UP_T^2 \sigma_{x,i}^2 \quad (21)$$

$$\langle \Delta E_k \rangle_L = \frac{\langle \Delta p_z^2 \rangle}{2m} \cong \gamma^4 UP_L^2 \sigma_{z,i}^2 \quad (22)$$

By comparing the potential energy with the change in kinetic energy, we obtain a rough estimate for the number of particles at which space charge effects become dominant

$$N \sim \frac{20\pi\epsilon_0 R}{3e^2} \langle \Delta E_k \rangle \quad (23)$$

For a 100 keV electron bunch with  $\sigma_{x,i} = \sigma_{z,i} = 1$  mm which is focused to a sphere with  $R \sim 5$   $\mu\text{m}$ , we find that the change in kinetic energy and the potential energy of the bunch become comparable for  $N \sim 10^4$  in case of a focusing power of  $P = 5$   $\text{m}^{-1}$ . For the given conditions, we can conclude from this rough estimate that bunches with  $N < 10^4$  are mainly limited in focusability by their emittance, while bunches with  $N > 10^4$  are mainly limited by space charge effects.

## 4.3. Synchronization and phase stability requirements

It is essential to have an accurate control over the phase of the field in the cavity. If a femtosecond laser is used in an ultrafast experiment for photoemission of electrons and/or for excitation of a sample in a pump-probe experiment, the RF source which drives the cavity needs to be synchronized with the laser. The application of a  $\text{TM}_{010}$  cavity in ultrafast time-resolved experiments puts some stringent requirements on the phase stability of the synchronization. Phase jitter in the RF signal that is used to drive the cavity and drift of the resonant frequency due to temperature changes in the cavity lead to changes in arrival time of the electron bunches with respect to the laser pulses. Both jitter and drift need to be sufficiently small.

In case of optimal compression ( $\phi_0 = \pi/2$ ), a relation between longitudinal momentum fluctuations  $\Delta p_z$  and phase fluctuations  $\Delta\phi_0$  can be derived from Eq. (13)

$$\Delta p_z \cong \frac{eE_0 d_c}{v_z} \Delta\phi_0 \quad (24)$$

A distance  $L$  behind the cavity, these phase fluctuations would lead to arrival time fluctuations  $\Delta t$  of

$$\Delta t = \Delta \left( \frac{L}{v_z} \right) \cong -L \frac{\Delta v_z}{v_z^2} = -L \frac{\Delta p_z}{m_e \gamma^3 v_z^2} = -L \frac{P_L}{\omega} \Delta\phi_0 \quad (25)$$

The relation between phase fluctuations and frequency fluctuations  $\Delta\omega$  is given by

$$\phi_0 = \arctan \left( 2Q \frac{\Delta\omega}{\omega} \right) \cong 2Q \frac{\Delta\omega}{\omega} \quad (26)$$

where  $Q$  is the unloaded quality factor of the cavity. For a 3 GHz  $\text{TM}_{010}$  cavity, typically  $Q \sim 10^4$ . When  $L = f_L = 1/P_L$ , the following simple expression is obtained

$$\Delta t \cong - \frac{2Q\Delta\omega}{\omega^2} \quad (27)$$

Using Eq. (27), we can derive stability requirements for the synchronization. For a cavity with  $Q = 10^4$  and  $\omega/2\pi = 3$  GHz, the arrival time fluctuations are  $\Delta t \cong (\Delta\omega/\omega) \times 10^{-6}$  s. If the requirement is  $\Delta t < 10$  fs, this implies  $\Delta\omega/\omega < 10^{-8}$ . For phase jitter within the frequency range of 0.05 Hz–100 kHz, this requirement can be achieved using a synchronization system developed in our group [21].

Temperature changes cause expansion or contraction of a cavity, leading to shifts of the resonant frequency. For a pillbox cavity, the frequency shift is given by [22]

$$\frac{\Delta\omega}{\omega} = -\kappa_T \Delta T \quad (28)$$

where  $\kappa_T$  is the thermal expansion coefficient, which is  $\kappa_T = 1.64 \times 10^{-5}$   $\text{K}^{-1}$  for copper [23]. The requirement  $\Delta\omega/\omega < 10^{-8}$  is for a copper cavity equivalent to the requirement that  $\Delta T < 0.6$  mK. A temperature stability of  $\Delta T < 1$  mK has been achieved in our lab for cavities with a power of 35 W through insulating the cavity and using a temperature control system.

## 5. Conclusions

Elementary closed expressions have been derived for the transverse and the longitudinal focusing powers of a  $\text{TM}_{010}$  microwave cavity. The applicability and accuracy of the derived equations have been validated by particle tracking simulations using realistic cavity fields. For small field amplitudes, in which case the “weak lens” approximation (given in Section 2.1) holds, the focusing powers obtained from simulations are in good agreement with the derived expressions. For larger field amplitudes, when the weak lens

assumption is not strictly valid anymore, clear discrepancies between the results from the theoretical expressions and simulations are observed. The derived expressions provide valuable insight into the beam dynamics and they are useful tools for designing beam lines.

## Acknowledgments

This research is supported by the Dutch Technology Foundation STW, applied science division of NWO and the Technology Program of the Ministry of Economic Affairs.

## Appendix. Resonant cavity – field expansion

A resonant cavity oscillating in a transverse magnetic (TM<sub>0nm</sub>) mode sustains an electric field

$$\vec{E}(\vec{r}, t) = \vec{E}_0(\vec{r}) \cos(\omega t + \phi_0) \quad (\text{A.1})$$

oscillating at an angular frequency  $\omega$  with a phase offset  $\phi_0$ . The electric field is cylindrically symmetric:  $\vec{E} = E_r \vec{e}_r + E_z \vec{e}_z$ . From Maxwell's equations, it then follows that the magnetic field only has an azimuthal component,  $\vec{B} = B_\phi \vec{e}_\phi$ . Both  $E_r$  and  $B_\phi$  are fully determined by  $E_z$

$$E_r = -\frac{1}{r} \int_0^r r' \frac{\partial E_z}{\partial z} dr' \quad (\text{A.2})$$

$$B_\phi = \frac{1}{rc^2} \int_0^r r' \frac{\partial E_z}{\partial t} dr' \quad (\text{A.3})$$

Because of the cylindrical symmetry, the amplitude of  $E_z$  can be expressed as

$$E_{0,z}(r, z) = \sum_{n=0}^{\infty} r^{2n} a_{2n}(z) \quad (\text{A.4})$$

where  $a_0(z) = E_{0,z}(r=0, \phi=0, z)$  is the amplitude of the on-axis longitudinal electric field. Using the fact that  $E_{0,z}$  obeys the Helmholtz equation, the following relation between the coefficients  $a_{2n}$  is obtained

$$a_{2n+2}(z) = -\frac{1}{(2n+2)^2} \left\{ \frac{\partial^2}{\partial z^2} + \frac{\omega^2}{c^2} \right\} a_{2n} \quad (\text{A.5})$$

By combining Eqs. (A.2–A.5), it is found that the electromagnetic field in the resonant cavity is fully determined by the on-axis field

profile  $E_{0,z}(z)$  and its derivatives

$$E_z(\vec{r}, t) = \left( 1 - \frac{r^2}{4} \left\{ \frac{\partial^2}{\partial z^2} + \frac{\omega^2}{c^2} \right\} + \dots \right) E_{0,z}(z) \cos(\omega t + \phi_0) \quad (\text{A.6})$$

$$E_r(\vec{r}, t) = \left( -\frac{r}{2} + \frac{r^3}{16} \left\{ \frac{\partial^2}{\partial z^2} + \frac{\omega^2}{c^2} \right\} - \dots \right) \frac{\partial E_{0,z}(z)}{\partial z} \cos(\omega t + \phi_0) \quad (\text{A.7})$$

$$B_\phi(\vec{r}, t) = \left( -\frac{r}{2} + \frac{r^3}{16} \left\{ \frac{\partial^2}{\partial z^2} + \frac{\omega^2}{c^2} \right\} - \dots \right) E_{0,z}(z) \frac{\omega}{c^2} \sin(\omega t + \phi_0) \quad (\text{A.8})$$

## References

- [1] J.M. LeBeau, S.D. Findlay, L.J. Allen, S. Stemmer, *Nano Letters* 10 (2010) 4405–4408.
- [2] B.J. Siwick, J.R. Dwyer, R.E. Jordan, R.J. Dwayne Miller, *Science* 302 (2003) 1382–1385.
- [3] R. Srinivasan, V.A. Lobastov, C.-Y. Ruan, A.H. Zewail, *Helvetica Chimica Acta* 86 (2003) 1763–1838.
- [4] W.E. King, G.H. Campbell, A. Frank, B. Reed, J.F. Schmerge, B.J. Siwick, B.C. Stuart, P.M. Weber, *Journal of Applied Physics* 97 (2005) 111101.
- [5] J.R. Dwyer, C.T. Hebeisen, R. Ernstorfer, M. Harb, V.B. Deyirmenjian, R.E. Jordan, R.J. Dwayne Miller, *Philosophical Transactions of the Royal Society of London Series A* 364 (2006) 741–778.
- [6] A.H. Zewail, *Science* 328 (2010) 187–193.
- [7] P. Musumeci, J.T. Moody, C.M. Scoby, M.S. Gutierrez, M. Westfall, R.K. Li, *Journal of Applied Physics* 108 (2010) 114513.
- [8] M. Eichberger, H. Schäfer, M. Krumova, M. Beyer, J. Demsar, H. Berger, G. Moriena, G. Sciani, R.J. Dwayne Miller, *Nature* 468 (2010) 799–802.
- [9] B.J. Siwick, J.R. Dwyer, R.E. Jordan, R.J. Dwayne Miller, *Journal of Applied Physics* 92 (2002) 1643–1648.
- [10] B.W. Reed, *Journal of Applied Physics* 100 (2006) 034916.
- [11] A.M. Michalik, J.E. Sipe, *Journal of Applied Physics* 99 (2006) 054908.
- [12] J.A. Berger, W.A. Schroeder, *Journal of Applied Physics* 108 (2010) 124905.
- [13] T. van Oudheusden, E.F. de Jong, S.B. van der Geer, W.P.E.M. Op 't Root, O.J. Luiten, B.J. Siwick, *Journal of Applied Physics* 102 (2007) 093501.
- [14] T. van Oudheusden, P.L.E.M. Pasmans, S.B. van der Geer, M.J. de Loos, M.J. van der Wiel, O.J. Luiten, *Physics Review Letters* 105 (2010) 264801.
- [15] L.C. Oldfield, *Microwave cavities as electron lenses*, PhD Thesis, University Library Cambridge, 1973.
- [16] L.C. Oldfield, *Journal of Physics E – Scientific Instruments* 9 (1976) 455–463.
- [17] O. Scherzer, *Zeitschrift für Physik* 101 (1936) 593–603.
- [18] T.P. Wangler, *RF Linear Accelerators*, John Wiley & Sons Inc., New York, 1998.
- [19] General Particle Tracer (GPT) code by Pulsar Physics, <<http://www.pulsar.nl>>.
- [20] M. Reiser, *Theory and Design of Charged Particle Beams*, second ed., Wiley-VCH Verlag GmbH & Co. KGaA, Weinheim, 2008.
- [21] F.B. Kiewiet, A.H. Kemper, O.J. Luiten, G.J.H. Brussaard, M.J. van der Wiel, *Nuclear Instruments & Methods A* 484 (2002) 619–624.
- [22] T. van Oudheusden, *Electron source for sub-relativistic single-shot femtosecond diffraction*, PhD Thesis, Eindhoven University of Technology Library, 2010.
- [23] *Handbook of Chemistry and Physics*, <<http://www.hbcpnetbase.com>>.